GNSS Multipath Detection in Urban Environment Using 3D Building Model

Shiwen Zhang, Sherman Lo, Yu-Hsuan Chen, Todd Walter, Per Enge
Aeronautics and Astronautics
Stanford University
Stanford, United States

***Abstract*—The paper describes a multipath detection algorithm to predict and exclude multipath signals using a ray-tracing algorithm on a three-dimensional building model. In addition, a sensitivity analysis was performed to estimate the confidence level of the model's multipath prediction. A field test was performed and experimental results showed that the detection accuracy using a building model is sensitive to both the modeling uncertainty and the accuracy of the initial user position estimate. Position accuracy was improved after applying the proposed detection algorithm.**

Keywords—multipath; urban navigation; 3D maps; ray tracing; satellite exclusion

I. INTRODUCTION

Multipath in Global Navigation Satellite Systems (GNSS) refers to the phenomenon when the satellite signals are reflected before reaching the user receiver. Such reflections can cause significant error in user's navigation solution. Multipath is a significant source of error in the urban environment. Identifying and reducing the effect of multipath would enable GNSS to be a primary component of high integrity railway control [1] and autonomous vehicle operating in urban environments.

Many studies have been conducted on GNSS multipath detection and mitigation. A multi-antenna system using a set of five antennas was proposed to estimate and remove multipath error based on the spatial correlation of received signals [2]. But this type of system is expensive and large in size, which makes it difficult to be implemented in commercial ground vehicles. A multipath detection technique based on satellite exclusion was introduced in [3] by using an upward-viewing infrared camera to identify the open sky. Satellites that are blocked by buildings, thus resulting in non-line-of-sight (NLOS) signals, were discarded when calculating position solutions. But this technique cannot reliably detect the case when both the line-of-sight (LOS) signal and the reflected signals arrive at the receiver.

Multipath detection methods using 3-dimensional (3D) environmental building model have also been heavily studied. Given that such maps are quickly being derived for urban environments, it make sense to use such models to aid GNSS integrity. One such method uses a simple building model derived from elevation-enhanced maps to predict NLOS signal propagation [4]. In [5], the authors incorporated the ray-tracing model with GPS/INS data fusion to reduce multipath error. And the authors in [6] simulated both LOS and NLOS signals through ray tracing and took into account the uncertainty of the building model.

Range redundancy checks such as receiver autonomous integrity monitoring (RAIM) can also detect and exclude multipath signals in processing. However, redundancy checks are suitable for situations where there are relatively few faulted (multipath affected or NLOS) signals relative to overall signals. While this is an appropriate assumption for an aircraft in flight, a deep urban canyon may have as many or more multipath and NLOS signals as clean LOS signals.

This paper describes and examines a multipath detection algorithm followed by satellite exclusion. The proposed algorithm uses a ray-tracing algorithm on a 3D building model to predict the signal paths at the estimated user position. This leverages building models and perhaps allows us a way of providing integrity in situations that may overwhelm the detection capabilities of RAIM. We have to be cognizant of the fact that the building models are not perfect and so sensitivity analysis on the building model is performed. This not only helps understand how imprecision in our knowledge may affect detection but also provides a potentially useful mechanism to estimate the confidence level of the prediction. Satellite exclusion is then executed based on the various prediction from our ray-tracing model and sensitivity analysis.

II. MODELING AND SIMULATION

The proposed multipath detection algorithm starts with ray tracing to predict the presence of both LOS and reflected signals given a satellite-user geometry. A 3D building model was developed for ray-tracing simulation and multipath prediction. The site chosen for simulation and testing is the Engineering Quadrangle (Quad) at Stanford University (Fig. 1). This site contains four buildings and each building is three-story high. The building model was constructed using building corner coordinates and building heights estimated from Google Earth. Detail structure of the building walls and roofs were not captured in the model to simplify the simulation. Trees and other foliage were also not modeled for the same reason. The final building model contains the surface normal vector and the boundaries of each sidewall for all the buildings in the model.

978-1-5386-1647-5/18/$31.00 ©2018 IEEE

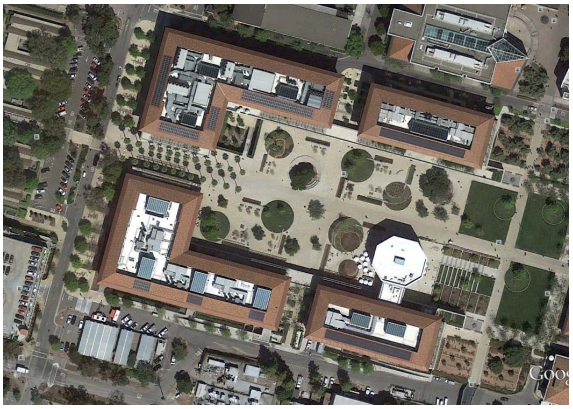

(a)

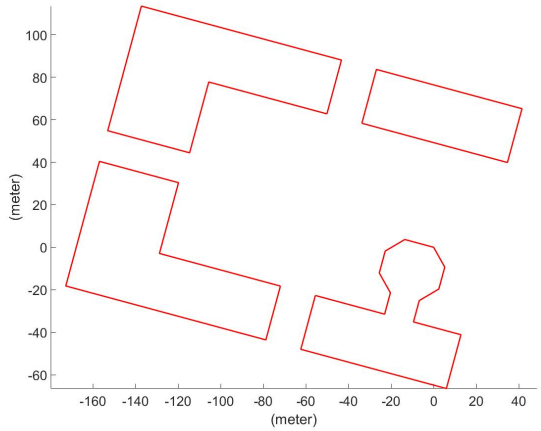

(b)

Fig. 1. (a) Top view of the simulation and testing site at Stanford University; (b) Building model created from Google Earth for simulation.

The ray-tracing algorithm simulates the LOS signal path as well as all the building-reflected signal paths from the satellite to the user receiver. The LOS propagation is simulated by a straight line segment connecting the satellite and the user receiver. Then the algorithm checks whether the propagation line passes through any sidewall within its boundaries. Single reflections are simulated using a vector-based ray-tracing method described in [7]. First of all, the satellite-user geometry is used to eliminate reflection surfaces. Sidewalls that are facing the wrong direction are discarded before further simulation for reflection path. And for each of the potential reflection surfaces, a reflection image of the user receiver with respect to the surface is generated. A propagation from the satellite to the receiver's image is then simulated. If this propagation path intersects with the reflection surface corresponding to the receiver image within its boundaries, the actual reflection path from the satellite to the receiver will be simulated. And if this reflection path is not blocked by any other sidewall, the reflection path will be stored for further calculation. The algorithm continues to find valid reflection paths from all possible reflection surfaces given the satellite-user geometry.

Ground reflection was not simulated since it is assumed that the GNSS antennas can effectively reject signals arriving at low or negative elevation angles. Simulations also showed that double reflection was likely not present in the specific environment. Other simulations also showed that multipath range error caused by diffraction is minimal and can be neglected. Therefore, diffraction and double reflection are both ignored in simulations used to generate model prediction on the experimental data.

Fig. 2 shows the simulation result for a satellite at 90-degree azimuth and 15-degree elevation. Fig. 2a shows the prediction of LOS coverage and Fig. 2b shows the regions where the received signal will be corrupted by signal reflections. The strip pattern in Fig. 2c is the result of interference between LOS signal and reflected signals. And when LOS signal is absent, reflected signals caused large range error in some regions shown in Fig. 2c.

III. Sensitivity Analysis

The ray-tracing algorithm is a deterministic algorithm. The prediction result is dependent on the accuracy of the building model and the assumed user location used in simulation. These are related in ray tracing as we care about the relative relationship between the user location and building walls. Therefore, to improve the robustness of the algorithm against building model uncertainty, a statistical sensitivity analysis with the ray-tracing algorithm was performed whereby building corner and height locations are taken as variable.

Independent and identically distributed uniform noise based on our building model uncertainty was added to each of the building corner locations and heights. Monte Carlo simulation was then carried out on the model with noise for statistical analysis. By comparing the difference in prediction between the original model and the model with noise, sensitivity to modeling uncertainty at a particular user location for a particular user-satellite geometry can be estimated.

Therefore, sensitivity analysis helps quantify the confidence level of the model's multipath prediction under modeling uncertainty. Fig. 3 and Fig. 4 are the plots for probability of disagreement for LOS prediction and reflection prediction, respectively, for a satellite at 90-degree azimuth and 15-degree elevation. Simulation result shows that for a low elevation satellite, reflection prediction is more sensitive to modeling uncertainty than LOS prediction.

IV. Experimental Results

A field test was performed on the Engineering Quad at Stanford University. L1 C/A GPS data were collected at 13 ground locations on the Engineering Quad using a NovAtel ProPak-V3 GNSS receiver (Fig. 5). Carrier smoothing interval was set to 2 seconds, which is the lowest value allowed by the receiver. But since carrier smoothing cannot be turned off completely, some multipath effect, particularly rapidly varying ones, will be smoothed out to some extent. The data collection

time was chosen so that both NLOS and multipath receptions were predicted, based on the building model and satellite geometry, to be present at the test locations. In order to maintain the same satellite geometry during the entire time of data collection, only 10 seconds of data were collected at each location. And the entire data collection process was completed in 12 minutes. Thirty minutes of extended data collection was also conducted and data were processed using the precise point positioning (PPP) service provided by Natural Resources Canada (NRCan) to obtain the ground truth of the testing points. A sky plot of all the satellites in view at the time of the field test is shown in Fig. 6. There were a total of 10 GPS satellites in view.

A. GPS Data Processing

GPS L1 pseudorange data were post-processed to remove the common errors including ionospheric error, tropospheric error and satellite clock bias. Ionospheric error corrections were obtained from Wide Area Augmentation System (WAAS). Tropospheric errors were estimated using the WAAS tropospheric delay model [8].

B. Detection Algorithms

A total of five algorithms for satellite exclusion were implemented on the collected GPS L1 pseudorange data. Single point positioning solution was calculated at each testing location. The same positioning algorithm using unweighted least squares was applied to all detection algorithms [9].

1) The no exclusion algorithm: This algorithm uses all the received signals to calculate position solutions. This is the all in view solution.

2) The residual checking (RAIM) algorithm: This is the standard Receiver Autonomous Integrity Monitoring (RAIM) Fault Detection and Exclusion (FDE) algorithm based on consistency checking of pseudorange residuals. This algorithm excludes signals that are inconsistent with the rest sequentially until the remaining residuals are consistent with each other according to a specific threshold. The algorithm then uses the remaining signals for position solutions. The detection threshold for RAIM-FDE corresponds to a false alarm rate of 0.1. A detailed description and derivation of RAIM algorithm can be found in [10].

3) The hard exclusion algorithm: This algorithm excludes signals based on the building model's predictions of LOS and reflection. Satellite positions and an initial estimate of the user position were inputted into the model to generate a multipath prediction for each satellite in view. The initial user position is estimated from the no exclusion algorithm and the user height is estimated from the building model. The model outputs two parameters. The first parameter predicts the presence of the LOS signal. The second parameter predicts the presence of the reflection signals. The decision process of the hard exclusion algorithm is shown in Table 1. Only satellite signals considered usable are those with only LOS is predicted. All other cases are excluded as the measurement is considered containminated by multipath. This is an extreme case aimed

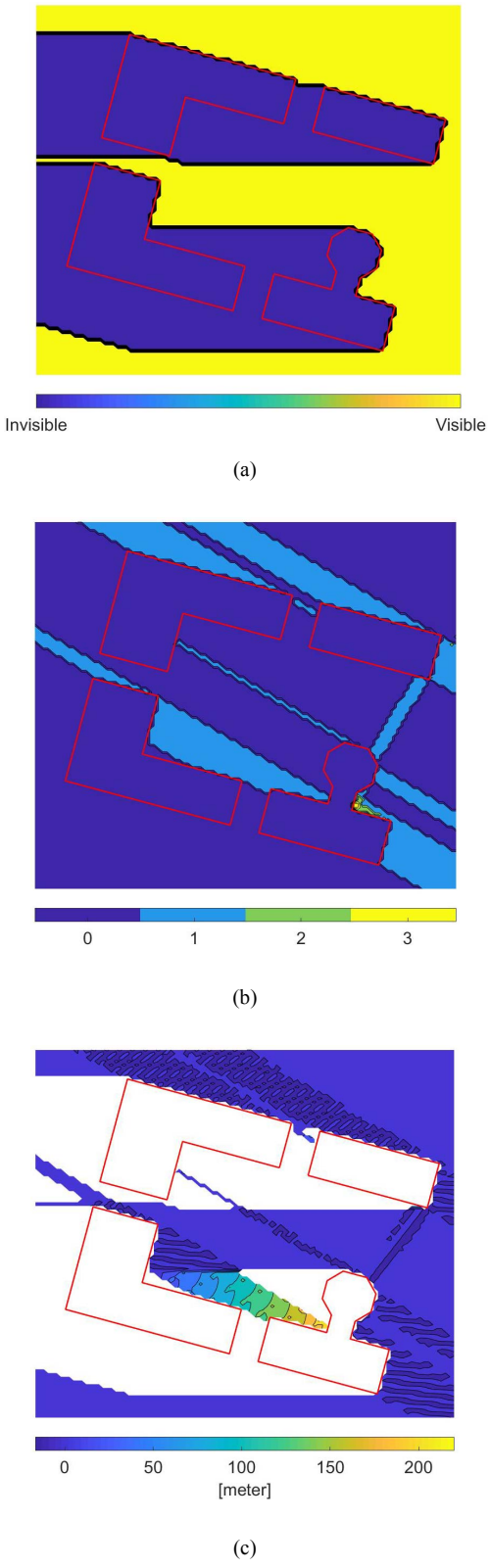

Fig. 2. (a) Line-of-signt coverage; (b) number of single reflections; (c) multipath range error. Modeled satellite signal is from 90 degree azimuth (North being zero degree) and 15 degree elevation.

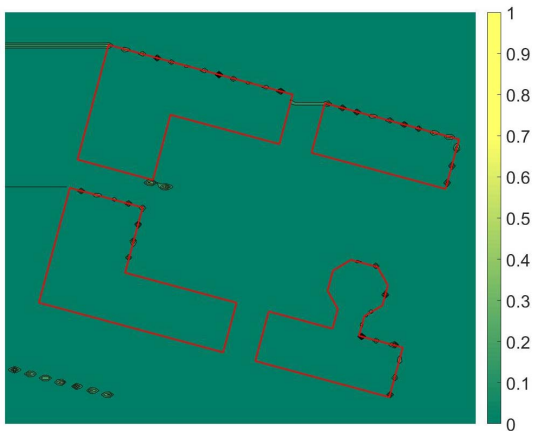

Fig. 3. Probability of disagreement for LOS prediction between the original model and the model with uncertainty for a satellite at 90-degree azimuth and 15-degree elevation.

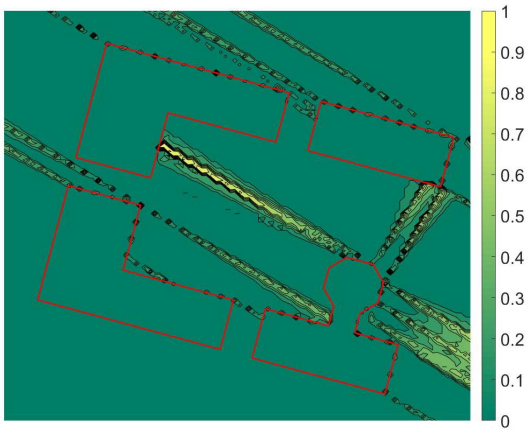

Fig. 4. Probability of disagreement for reflection prediction between the original model and the model with uncertainty for a satellite at 90-degree azimuth and 15-degree elevation.

Fig. 5. Field testing locations on the engineering quad.

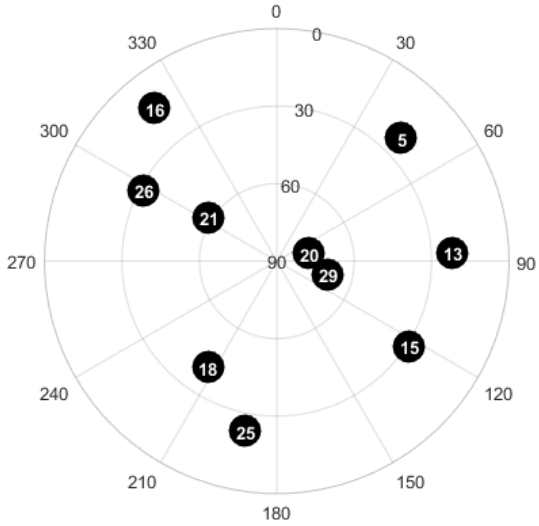

Fig. 6. Sky plot of all the satellites in view at the time of the field test.

at maximizing integrity. Certainly, the model can provide the multipath delay which provides an estimate of the its severity. This more granular information is not used but may be worth exploring in the future. Detection results from the hard exclusion algorithm showed that accurate detection of multipath signals based on the building model can be affected by two factors: the uncertainty in the model and the accuracy of the initial user position estimate. Therefore, two more detection algorithms were implemented to demonstrate the effect of each of these two factors on the model's detection accuracy.

4) The soft exclusion algorithm: The soft exclusion algorithm performs satellite exclusion based on uncertainty in the building model. Sensitivity analysis was performed at each testing location. Uniform noise with distribution U(-1 m, 1 m) was added to each of the building corner coordinates and building heights. Monte Carlo simulation was carried out for 100 times on the model. Two sensitivity parameters, one indicating the confidence level of the LOS prediction and the other indicating the confidence level of the reflection prediction, were generated by averaging over the simulation results. For example, if 30 out of the 100 simulations predict "yes' for LOS, the sensitivity parameter for LOS prediction is 0.3. The decision process of the soft exclusion algorithm is listed in Table 2. The table incorporates a basic notion of severity of the multipath in its decision threshold. The threshold for having a reflection result in excluding the satellite signal is higher if a LOS is believed to be present (prediction is "yes"). This is because multipath error is bounded when LOS signal is present, and error caused by worse satellite geometry may exceed the error caused by multipath in this case. This higher threshold is a representation of the tradeoff between multipath error and satellite geometry.

5) Hard exclusion initialized with RAIM (Hard + RAIM): This algorithm is the same hard exclusion algorithm as

described before. But instead of using the no exclusion algorithm to obtain an estimate of user position, the position estimate from the RAIM algorithm was used. So this algorithm allows us to examine the sensitivity of hard exclusion's detection performance to errors in initial position.. The position solution using RAIM is better in this multipath environment than that from the all in view.

TABLE I. EXCLUSION DECISION FOR THE HARD EXCLUSION ALGORITHM

LOS	Reflection	Decision
Yes	No	Include
Yes	Yes	Exclude
No	Yes	Exclude
No	No	Exclude

TABLE II. EXCLUSION DECISION FOR THE SOFT EXCLUSION ALGORITHM

Sensitivity analysis				Decision
Probability of LOS		*Probability of reflection*		
> 0.6	Yes	< 0.8	No	Include
> 0.6	Yes	> 0.8	Yes	Exclude
< 0.6	No	< 0.6	No	Exclude
< 0.6	No	> 0.6	Yes	Exclude

C. *Results and Discussion*

Performance of the five detection algorithms were evaluated. Fig. 7 shows the root mean squared (rms) 3D position error at each testing location for the five algorithms plotted against the distances to the first testing location. Position error from the no exclusion algorithm suggests that multipath was present at multiple testing locations with an extreme case at location 7. The hard exclusion algorithm removed several signals and reduced the large position errors that we believe to be due primarily to multipath signals. The performance of the hard exclusion algorithm at locations 3 and 13 was worse than the no exclusion algorithm. This is due to excluding so many signals that satellite geometry was significantly affected. The horizontal dilution of precision (HDOP) was calculated and plotted in Fig. 8. Comparing HDOP at locations 3 and 13 shows that the hard exclusion algorithm removed too many signals at these locations and caused poor satellite geometry.

Examination of the hard + RAIM results show much lower errors for locations 3 and 13 which suggests that the initial position error can have a significant effect. The no exclusion and RAIM algorithm both have similar levels of errors for those two locations. But they have different enough positions, as shown in Fig 9, to result in different decisions by the hard exclusion algorithm. Overall the hard + RAIM algorithm has low errors for all testing locations. Fig. 10 shows hard exclusion results using the true location for initial position. The errors for the hard + true algorithm are the same as the errors for the hard + RAIM algorithm, which indicates that the

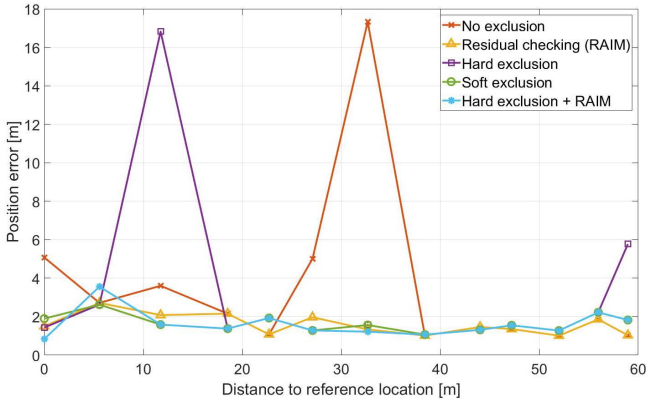

Fig. 7. Position error at each testing location for the five detection algorithms.

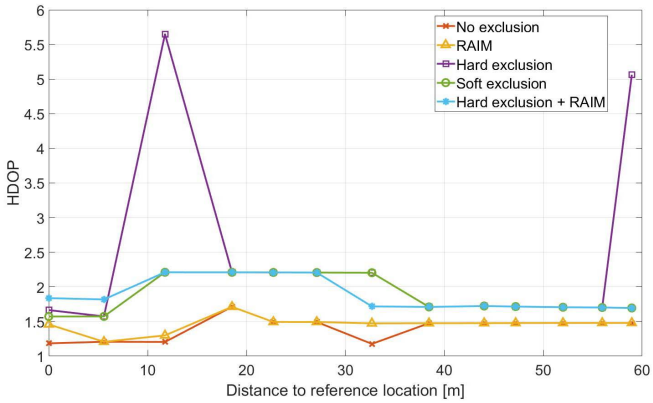

Fig. 8. Horizontal dilution of precision based on satellites used for position solution at each testing location for the five detection algorithms.

RAIM solution is close enough to the true location of the user for the hard exclusion algorithm to make consistent decisions.

The soft exclusion algorithm also produces solutions with consistently low errors. The uncertainty model in the soft exclusion is developed to handle building model uncertainty. But in doing that it also handles some initial position error.

V. CONCLUSION

This paper examined a multipath detection method that uses 3D building model. Experimental results show that the detection performance of the model depends on the initial user position estimate as well as modeling uncertainty. The current results do not indicate whether it is the building model or initial user position error that is the cause, though the hard exclusion results suggest that the latter was causing the large errors found. The algorithm that addresses initial position error and the algorithm that addresses the building model

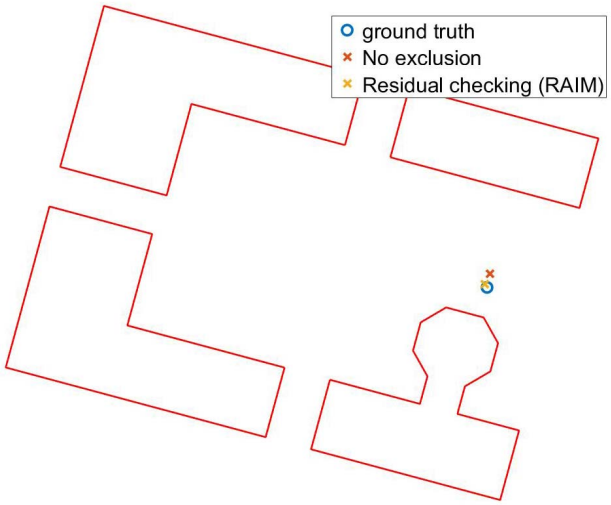

Fig. 9. 2D position plot of ground truth, no exclusion solution, and RAIM solution for testing lcoation 3.

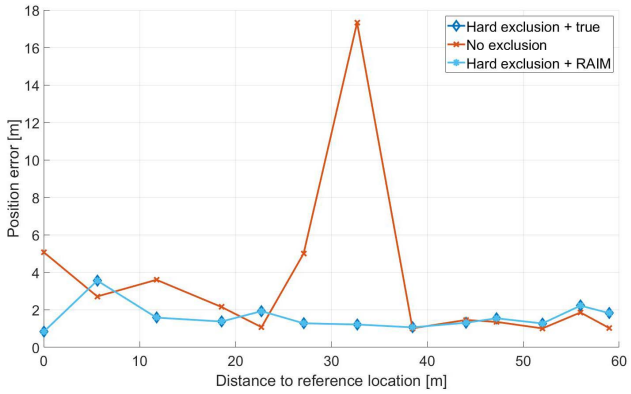

Fig. 8. Position error at each testing location for the no exclusion algorithm, the hard + RAIM algorithm, and the hard + true algorithm.

uncertainty relative to the user location both greatly improved the position solution, demonstrating the importance of handling these uncertainties.

The results show that a building model perform as well as RAIM in mitigating multipath effects on position. This is significant as these building models can address some of the limitations in RAIM and other consistency checking algorithms for multipath detection. In particular, RAIM may not be able to detect multipath signal when multiple signals with large multipath error are present in the measurements. A detection method based on building model can be used to either crosscheck RAIM's detection result or provide additional information to RAIM algorithm for multipath detection. Further analysis and more experimental data are needed to validate the model and to evaluate the effectiveness of the method. And the dilemma of requiring an accurate user position estimate to improve the model's detection performance still needs to be addressed.

REFERENCES

[1] A. Neri, F. Rispoli and P. Salvatori, "A GNSS based solution for supporting virtual block operations in train control systems," *2015 International Association of Institutes of Navigation World Congress (IAIN)*, Prague, 2015, pp. 1-6.

[2] J. K. Ray, M. E. Cannon and P. Fenton, "GPS code and carrier multipath mitigation using a multiantenna system," in *IEEE Transactions on Aerospace and Electronic Systems*, vol. 37, no. 1, pp. 183-195, Jan 2001.

[3] J. i. Meguro, T. Murata, J. i. Takiguchi, Y. Amano and T. Hashizume, "GPS Multipath Mitigation for Urban Area Using Omnidirectional Infrared Camera," in *IEEE Transactions on Intelligent Transportation Systems*, vol. 10, no. 1, pp. 22-30, March 2009.

[4] C. Piñana-Diaz, R. Toledo-Moreo, D. Bétaille and A. F. Gómez-Skarmeta, "GPS multipath detection and exclusion with elevation-enhanced maps," *2011 14th International IEEE Conference on Intelligent Transportation Systems (ITSC)*, Washington, DC, 2011, pp. 19-24.

[5] M. Obst, S. Bauer and G. Wanielik, "Urban multipath detection and mitigation with dynamic 3D maps for reliable land vehicle localization," *Proceedings of the 2012 IEEE/ION Position, Location and Navigation Symposium*, Myrtle Beach, SC, 2012, pp. 685-691.

[6] S. Miura, S. Hisaka and S. Kamijo, "GPS multipath detection and rectification using 3D maps," *16th International IEEE Conference on Intelligent Transportation Systems (ITSC 2013)*, The Hague, 2013, pp. 1528-1534.

[7] L. Lau, and P. Cross, "Development and testing of a new ray-tracing approach to GNSS carrier-phase multipath modelling," *Journal of Geodesy*, vol. 81, no. 11, pp. 713, 2007.

[8] WAAS MOPS, Minimum Operational Performance Standards for Global Positioning System/Wide Area Augmentation System Airborne Equipment, RTCA Inc. Document No. RTCA/DO-229D, December 13, 2006.

[9] P. Misra, and P. Enge. *Global Positioning System: signals, measurements and performance second edition*. Lincoln, MA: Ganga-Jamuna Press, 2006.

[10] J. Blanch, T. Walter, and P. Enge. "Advanced RAIM User Algorithm Description: Integrity Support Message Processing, Fault Detection, Exclusion, and Protection Level Calculation," *Proceedings of the 25th*.